FORCES CALCULATION METHOD OF THOMPSON LEVITATING RING DURING ITS NON-HARMONIC FEEDING

[*]Daniel VACHTL, [**]Dobroslav KOVÁČ, [*]Daniel MAYER
[*]Department of Theory of Electrical Engineering, Faculty of Electrical Engineering, University of West Bohemia in Pilsen, Univerzitní 26, 306 14 Plzeň, Czech Republic, E-mail: dvachtl@kte.zcu.cz, mayer@kte.zcu.cz
[**] Department of Theoretical Electrotechnics and Electrical Measurement, Faculty of Electrical Engineering and Informatics, Technical University of Košice, Letná 9, 042 00 Košice, Slovak Republic, E-mail: dobroslav.kovac@tuke.sk

SUMMARY

The work represents a contribution to a part of graduate course devoted to magnetic levitation. It deals with computation of electromagnetic levitation force acting on the Thompson ring in case of its steady state non-harmonic feeding. The theoretical analysis was verified on a demonstration device in common with simulation of its magnetic parameters. The results obtained on the basis of theoretical and simulation analyses were validated by measurement.

Keywords: *magnetic levitation, Thompson ring, pulse actuator*

1. INTRODUCTION

Magnetic levitation (maglev) may be defined as hovering of a solid body caused by force effects of electromagnetic field. It can be based on several physical principles. In the last forty years the effect was intensively investigated and there exist several technical domains in which it can successfully be exploited. Mentioned may be particularly the super express vehicles that reach velocities up to 550 km/h, magnetic bearings used for high-revolution applications (up to 200000 min^{-1}) and contactless induction melting, when the molten metal is not in contact with the crucible wall.

A specific category includes levitation devices such as pulse actuators, whose principle is used in electromagnetic guns, release devices in fast circuit breakers etc. One of the first devices of this kind is the so called Thompson jumping ring schematically depicted in Fig. 1. Elihu Thompson carried out the first experiment with the device in 1887. Its history is described in works [1] and [7]. It consists of a coil, magnetically soft ferromagnetic rod core and nonferromagnetic electrically well conductive ring put on the core. As some modern pulse actuators are based on the principle of the Thompson jumping ring, the presented study is devoted to the theory and construction of a corresponding demonstration device. The device will serve as an educational aid for teaching of magnetic levitation in subject electrodynamics.

The Thompson ring works in the following way: the coil is supplied by a current pulse (for example discharge current from a connected capacitor) that produces pulse magnetic field. Current generated in the ring interact with the original magnetic field, which results in levitation force launching the ring up.

In the investigated case the non-harmonic current delivered from an alternating voltage converter was used. The ring is then affected not by a single force pulse, but by pulsating force that brings about, in common with other dynamic properties of the ring (inertia and friction in ambient air) its levitation.

The mentioned experimental device allows feeding of the system from a network transformer, without necessity of construction of an expensive and complicated converter. For practical realization it may be used only the cheap and simple AC/AC converter.

Low network frequency (50 Hz) allows, moreover, neglecting of skin effects in the field coil, which simplifies solution of magnetic field.

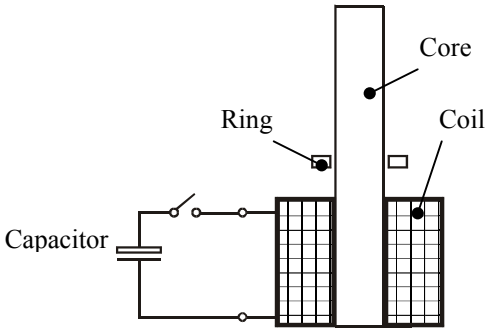

Fig. 1 A pulse actuator

2. MATHEMATICAL MODEL

2.1. Definition area

Magnetic field was solved by FEM-based code QuickField in cylindrical coordinate system (r, z). The definition area is depicted in Fig. 2.

The code solves harmonic steady state. For non-harmonic current the superposition for particular components is used.

Steady-state harmonic magnetic field can be described in terms of the phasor of magnetic vector potential $\boldsymbol{A}$ that may be expressed as:

$$\overline{\boldsymbol{A}} = \mathbf{r}^0\overline{A}_\mathrm{r} + \boldsymbol{\alpha}^0\overline{A}_\alpha + \mathbf{k}\overline{A}_\mathrm{z} \qquad (1)$$

In our case the only nonzero component is the tangential component $\overline{A}_\alpha$, so that:

$$\overline{\boldsymbol{A}} = \boldsymbol{\alpha}^0 \overline{\boldsymbol{A}}_\alpha \tag{2}$$

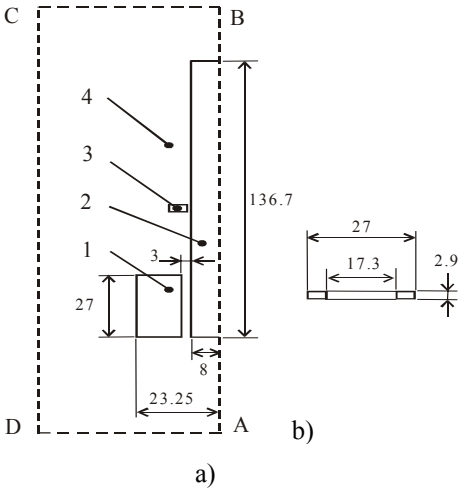

Fig. 2 a) Definition area
b) Dimensions of the aluminum ring

2.2. Equation of harmonic magnetic field

Time variable magnetic field is generally described by equation:

$$\Delta \boldsymbol{A} - \mu\varepsilon \frac{\partial^2 \boldsymbol{A}}{\partial t^2} - \mu\gamma \frac{\partial \boldsymbol{A}}{\partial t} = -\mu \boldsymbol{J}_{\mathrm{vn}} \tag{3}$$

that holds simultaneously with another equation:

$$\operatorname{div} \boldsymbol{A} + \mu\varepsilon \frac{\partial \varphi}{\partial t} + \mu\gamma\varphi = 0 \tag{4}$$

where $\boldsymbol{J}_{\mathrm{vn}}$ denotes current density of field currents and φ scalar electric potential.

Derivation of (3) is presented in a lot of textbooks on electromagnetic field theory, see, for instance [2]. For harmonic field currents the phasor modification of (3) can be used in form:

$$\Delta \overline{\boldsymbol{A}} + \overline{\boldsymbol{k}}^2 \overline{\boldsymbol{A}} = -\mu \overline{\boldsymbol{J}}_{\mathrm{vn}} \tag{5}$$

where

$$\overline{\boldsymbol{k}}^2 = \omega^2 \left(\varepsilon - \mathrm{j}\frac{\gamma}{\omega} \right) \mu = \omega\mu \left(\omega\varepsilon - \mathrm{j}\gamma \right). \tag{6}$$

Condition (4) then reads:

$$\operatorname{div} \overline{\boldsymbol{A}} + \mu \left(\gamma + \mathrm{j}\omega\varepsilon \right) \overline{\varphi} = 0 \,. \tag{7}$$

As far as the magnetic field can be considered quasistationary, then:

$$\overline{\mathrm{k}}^2 = -\mathrm{j}\omega\,\gamma\mu \,. \tag{8}$$

As mentioned above, equation (5) was solved by code QuickField.

2.3. Parameters of individual subregions

Subregion 1: The diameter of coil conductor is 0.8 mm, number of its turns $N = 184$, $\mu_{\mathrm{r}} = 1$, $\gamma = 0$.

If the conductivity $\gamma = 0$, the uniform distribution of current density is assumed (influence of skin effect is neglected).

Subregion 2: magnetically soft ferromagnetic material of parameters μ_{r}=370, $\gamma = 5 \times 10^6$ S/m.

Subregion 3: aluminum ring of parameters $\mu_{\mathrm{r}} = 1$, $\gamma = 3.7\mathrm{x}10^7$ S/m, mass m = 2.63 g.

Subregion 4: air, $\mu_{\mathrm{r}} = 1$, $\gamma = 0$.

2.4. Boundary conditions and conditions on interfaces

- Boundary A-B is characterized by antisymmetry, i.e. $\overline{\boldsymbol{A}} = 0$.
- Boundary B-C-D-A that is placed at a sufficient distance from the system represents a force line along which $\overline{\boldsymbol{A}} = 0$.
- The condition along the interface between subregions i, j reads:

$$\frac{1}{\mu_i} \frac{\partial \overline{\boldsymbol{A}}_i}{\partial \mathbf{n}_{ij}} = \frac{1}{\mu_j} \frac{\partial \overline{\boldsymbol{A}}_j}{\partial \mathbf{n}_{ij}} \tag{9}$$

where **n** is the normal vector to the interface oriented from subregion i to subregion j.

The finite element method satisfies the conditions along all interfaces automatically.

2.5. Forces in magnetic field

The force acting on the ring may be determined from the Maxwell tensor of stresses (for details see [2], [5]).

Program QuickField calculates this force from expression:

$$\boldsymbol{F} = \frac{1}{2} \cdot \oiint \left[\overline{\boldsymbol{H}} \left(\mathbf{n} \cdot \overline{\boldsymbol{B}} \right) + \overline{\boldsymbol{B}} \left(\mathbf{n} \cdot \overline{\boldsymbol{H}} \right) - \mathbf{n} \left(\overline{\boldsymbol{H}} \cdot \overline{\boldsymbol{B}} \right) \right] \mathrm{d}\,\boldsymbol{S} \,. \tag{10}$$

3. EXPERIMENTAL SOLUTION

The goal of the numerical solution was to find the lift of the ring as a function of the control angle of the triac regulator.

3.1. Determination of actuator parameters

First, the basic parameters of the feeding circuit were determined: harmonic input voltage U_2 of the converter, load (parameters L_{z} and R_{z}) and field current I_{z}. The network transformer of apparent output 60 VA with output voltage U_2 = 6.4 V was used.

The load is represented by the field coil with $N = 184$ turns and dimensions given in Fig. 2. Its

conductor is a copper wire of radius 0.8 mm. Its resistance is:

$$R_Z = \rho \frac{l}{S} = 0.3505 \ \ \Omega \tag{11}$$

Inductance L_z and current I_z are mutually dependent and this dependence is nonlinear due to the presence of ferromagnetic core. Both quantities may be found by successive approximations. The magnetization characteristic of the core is in Fig. 3.

The load current I_z was supposed 7.7A and relative permeability of the core μ_r=370.

These values were used for the numerical simulation of the actuator. The results are in Fig. 4.

Now the inductance L_z is:

$$L_z = \frac{NBS}{I} = \frac{184 \times 0.499698 \times \pi \times (0.008)^2}{7.7} = 2.4 \text{ mH} \tag{12}$$

The check of load current from L_z then provides:

$$I = \frac{U}{Z} = \frac{6.4}{\sqrt{(0.3501)^2 + (2\pi \times 50 \times 0.0024)^2}} = 7.69 \text{ A} \tag{13}$$

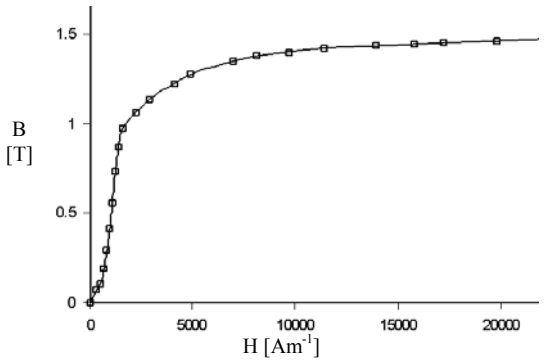

Fig. 3 Magnetization characteristic of the used steel

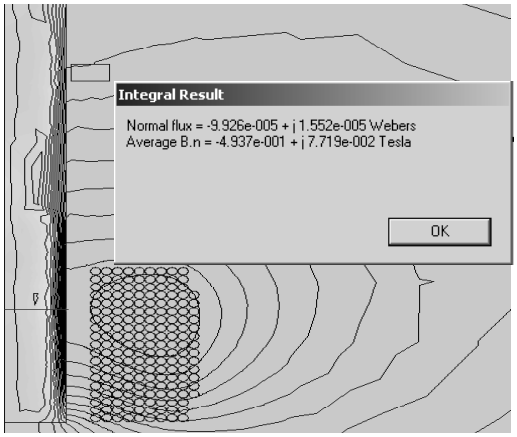

Fig. 4 Simulation of magnetic field of the actuator

The result shows that the original estimation of load current I_z was correct. Correct is then also the value of inductance L_z. Moreover, from Fig. 3 it is clear that the operation point moves in the linear part of the magnetization characteristic. And that is why this characteristic may be substituted by a constant value of magnetic permeability μ_r=370. Now the originally nonlinear problem may be handled as a linear one.

3.2. Computation of the levitation force acting on the ring

The average value of force for the prescribed lift was first determined for the case when the control angle α of the triac regulator was smaller or at best equal to angle φ of the phase shift between current and voltage of the load. In our case it was $\alpha = 65°$, when the coil carried sinusoidal current. Then the cases $\alpha = 90°$ and $\alpha = 105°$ was solved.

From the values of inductance L_z, resistance R_z and required control angles α (65°, 90°, 105°) the parameters of first nine harmonic components of the corresponding nonharmonic current I_z was determined (using program PSpice).

Then the average value of force acting on the ring in the position when the force superposition of all considered harmonic components was equal to its weight was calculated by QuickField program. The position of the ring was measured before, on the real device. The difference between the weight of the ring and calculated force for its given position and then the relative error was determined. In this way the results was validated.

3.3. Connection of the experimental device

The block scheme of the proposed connection is in Fig. 5. The alternating converter is realized by means of a triac regulator whose connection is in Fig. 6.

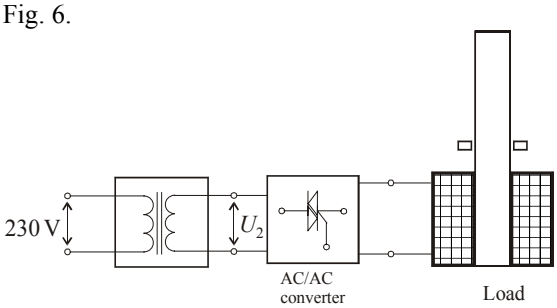

Fig. 5 Block scheme of the experimental device

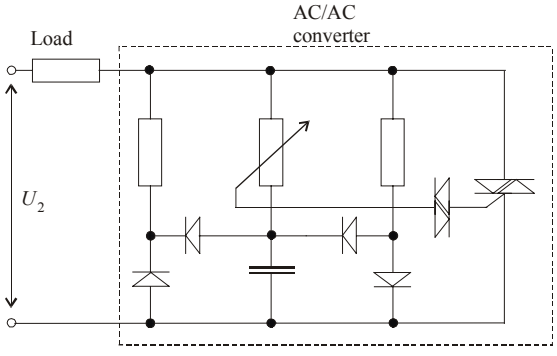

Fig. 6 Connection of the triac regulator

By control of the converter the field current and consequently, the levitation force acting on the ring can be varied.

3.4. Results

The simulation of the current and voltage waveforms and their harmonic analysis in PSPICE program was done first for the determined control angles. The results are listed in Figs. 7, 11, 14 and in Tabs. 1, 2 and 3.

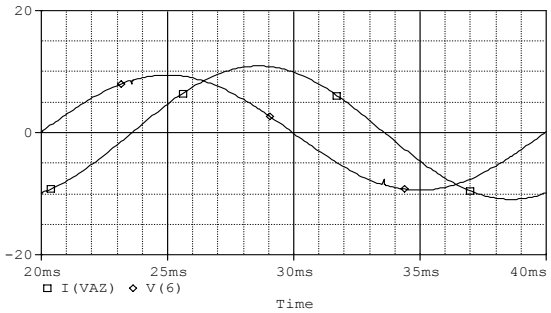

Fig. 7 Simulate waveforms for control angle $\alpha = 65°$

order of harmonic	frequency [Hz]	amplitude [A]	phase shift [deg]
1	50	1.0920E+01	-6.4660E+01
2	100	1.6630E-03	-1.1310E+02
3	150	3.1010E-03	-4.7150E+01
4	200	8.3800E-04	1.1040E+02
5	250	2.1800E-03	1.6990E+02
6	300	5.8390E-04	-1.8750E+01
7	350	1.6580E-03	3.7500E+01
8	400	4.2280E-04	-1.4520E+02
9	450	1.1790E-03	-8.9440E+01

Tab. 1 Decomposition of the current into harmonic components for $\alpha = 65°$

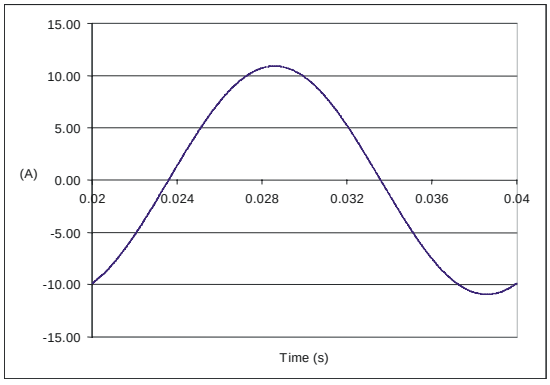

Fig. 8 The waveform of current obtained by synthesis of harmonic components for control angle $\alpha = 65°$

The verification waveforms of the load current obtained by synthesis of calculated harmonic components for particular control angles are given in Figs. 8, 12 and 15.

The waveforms of voltages and currents measured on the real device for various control angles are shown in Figs. 9, 13 and 16. The lift of the ring was measured for these angles. The result for control angle $\alpha = 65°$ is depicted in Fig. 10.

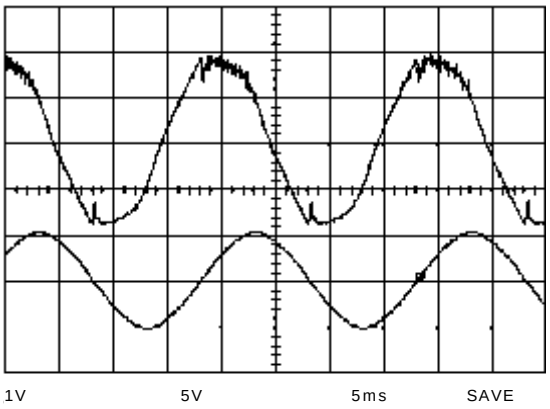

Fig. 9 Measured waveforms of u_z and i_z on the real device for control angle $\alpha = 65°$

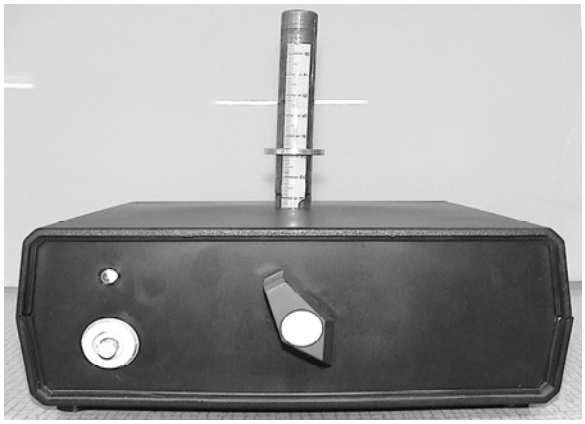

Fig. 10 Lift of the ring on the real device for control angle $\alpha = 65°$

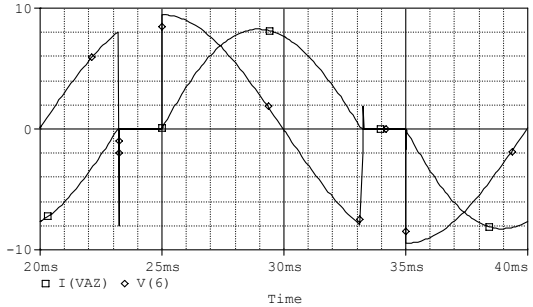

Fig. 11 Simulated waveforms for control angle $\alpha = 90°$

order of harmonic	frequency [Hz]	amplitude [A]	phase shift [deg]
1	50	7.4300E+00	-7.2470E+01
2	100	3.8010E-04	-2.4690E+01
3	150	1.2110E+00	-3.3640E+01
4	200	3.8020E-04	-1.3820E+02
5	250	5.7760E-01	1.7430E+02
6	300	3.7510E-04	1.0720E+02
7	350	2.7390E-01	2.3720E+01
8	400	3.7850E-04	-7.7590E+00
9	450	1.0170E-01	-1.2860E+02

Tab. 2 Decomposition of the current into harmonic components for $\alpha = 90°$

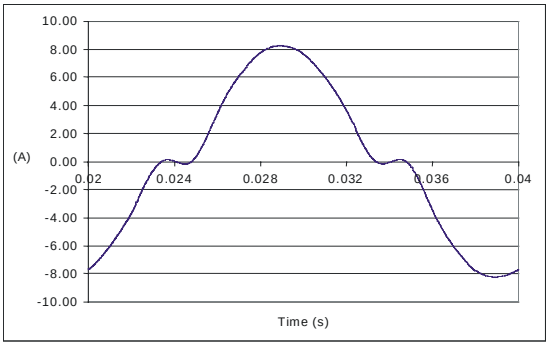

Fig. 12 The waveform of current obtained by synthesis of harmonic components for control angle $\alpha = 90°$

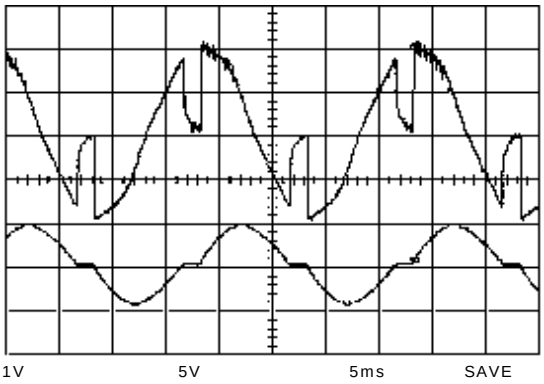

Fig. 13 Measured waveforms of u_z and i_z on the real device for control angle $\alpha = 90°$

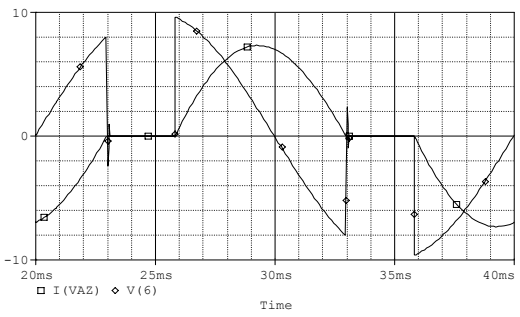

Fig. 14 Simulated waveforms for control angle $\alpha = 105°$

order of harmonic	frequency [Hz]	amplitude [A]	phase shift [deg]
1	50	6.0210E+00	-7.8140E+01
2	100	5.8080E-05	2.9030E+01
3	150	1.7400E+00	-5.2560E+01
4	200	4.3250E-05	-2.8070E+01
5	250	5.2560E-01	1.4260E+02
6	300	2.1070E-05	-7.3990E+01
7	350	3.5010E-02	-6.2640E+01
8	400	8.2410E-06	-3.4200E+01
9	450	1.3940E-01	1.2310E+01

Tab. 3 Decomposition of the current into harmonic components for $\alpha = 105°$

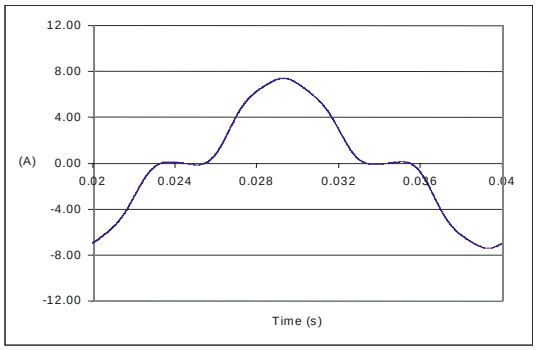

Obr. 15 The waveform of current obtained by synthesis of harmonic components for control angle $\alpha = 105°$

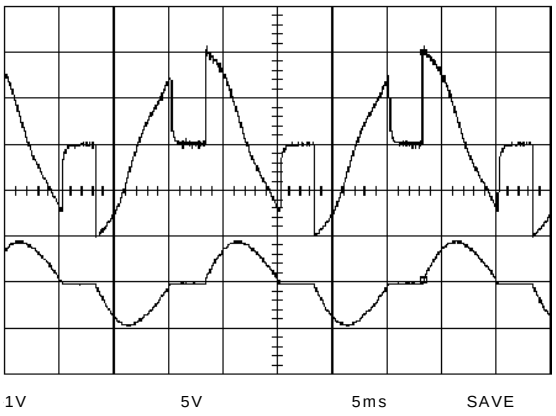

Obr. 16 Measured waveforms of u_z and i_z on the real device for control angle $\alpha = 105°$

The nine harmonic components of forces, which are listed in Tab. 4, were calculated by QuickField program for every control angle. The table also contains their sums and relative errors. The formulas used for computation of particular items are below the table.

Control angle [deg]	Lift of the ring [mm]	Harmonic components									ΣF [N]	ΔF [N]	δ [%]
		1.	2.	3.	4.	5.	6.	7.	8.	9.			
65	31.5	2.5277E-02	0	0	0	0	0	0	0	0	2.5277E-02	4.9700E-04	1.9283E+00
90	16.5	2.2017E-02	0	1.8089E-03	0	5.3310E-04	0	1.3040E-04	0	1.8607E-05	2.4508E-02	1.2665E-03	4.9139E+00
105	12	1.8125E-02	0	4.7664E-03	0	5.6685E-04	0	2.7628E-06	0	4.5255E-05	2.3506E-02	2.2677E-03	8.7985E+00

Tab. 4 Calculated values of forces from particular harmonics mass of the ring $m = 0.00263$ kg , $\Sigma F = \sum_{i=1}^{9} F_i$, weight of the ring $F_g = mg = m$ x 9.8 [m/s]= 0.025774 N, $\Delta F = \Sigma F - F_g$, $\delta = 100(\Sigma F - F_g)/F_g$

4. CONCLUSION

The hypothesis about possibility of determining levitation forces produced by nonharmonic current by superposition of individual harmonic components was validated on the proposed device. The calculated results are in a good accordance with measured data even when solution of the mathematical model was carried out under various simplifying assumptions. The method of determination of the lift at nonharmonic supply by means of the harmonic analysis proved to be suitable and sufficiently accurate.

The device with triac regulation allows levitating an aluminum ring within the range from zero to 31.5 mm with field current of RMS value changing from zero to 7.7A.

REFERENCES

[1] Barry, N. - Casey. R.: Elihu Thompson's Jumping Ring in a Levitated Closed-Loop Control Experiment. IEEE, Transaction on Education, Vol. 42, No. 1, Feb.1999, 72 045080.

[2] Haňka, L.: Theory of Electromagnetic Field. SNTL/ALFA, Praha, 1975 (in Czech).

[3] Kováčová, I. - Kováč, D.: Modeling of Converters. Textbook for FEI TU Košice, ELFA - Košice, 1997, 112 pages, (in Slovak).

[4] Kováčová, I. - Kováč, D. - Oetter, J.: Applied Electronics. Hint for Seminars, textbook, Košice, Akris, 2001, 94 pages, (in Slovak).

[5] Mayer, D.: Electrodynamics in Electrical Power Engineering. BEN, 2005, 280 pages, (in Czech).

[6] Mayer, D. - Jedlička, M.: Lift and Drag Forces on Magnetically Suspended Trains. Acta Technica CSAV, Vol. 49, 2004, pp. 137–147.

[7] Mayer, D. - Teplý, J.: Mathematical Model of Thompson Jumping Ring. Acta Technica CSAV, Vol. 66, 2000, pp. 137–149.

[8] Šimko, V. - Kováč, D. - Kováčová, I.: Theoretical Electroengineering II. Elfa s.r.o., Košice 2000, 168 pages, (in Slovak).

BIOGRAPHIES

Daniel Vachtl (Ing.) was born in Czech Republic in 1980. In 2004 he graduated in the study field of the Construction of electrical machines and instruments at the University of West Bohemia, Faculty of Electrical Engineering, Pilsen, Czech Republic. At present he is PhD student at the Department of Theory of Electrical Engineering, University of West Bohemia, Pilsen, Czech Republic. His teaching and research activities include electromagnetic field theory, circuits theory and magnetic levitation.

Kováč Dobroslav - He finished his studies in 1985 at the Technical University of Košice, Department of Electrical Drives, area - Power electronics with excellent evaluation. Then he worked as a research worker at the Department of Electrical Drives. His research work was focused on the practical application of new power semiconductor devices. In 1989 he got the Award of the Minister of Education for the Development of Science and Technology. From 1991 he has worked as assistant lecturer at the Department of Theoretical Electrical Engineering and Electrical Measurement. He got his doctoral diploma in 1992 for the work on the field of power electronics. From 2000 he has worked as professor and his working interest is now focused mainly on the field of computer simulation of power electronic circuits and automated computer measuring.

Daniel Mayer (Prof., Ing., PhD., DrSc.) was born in Pilsen, Czech Republic in 1930. He received the Ing., PhD. and DrSc. degrees in electrical engineering from Technical University of Prague in 1952, 1958 and 1979, respectively. In 1956 he began his professional career as a Senior Lecturer and later as a Associate Professor at the University of West Bohemia in Pilsen. In 1968 he was appointed Full Professor of the Theory of Electrical Engineering. Many years he has been head of the Institution of Theory of Electrical Engineering. His main teaching and research interests include circuit theory, electromagnetic field theory, electrical machines and history of electrical engineering. He has published 6 books and more than 240 scientific papers. He is a Fellow of the IEE, member ICS, ISTET and UICEE, member of editorial boards of several international journals and leader of many grant projects.